

Stochastic theory of non-equilibrium wettingF. DE LOS SANTOS^{1,3}, M.M. TELO DA GAMA¹, AND MIGUEL A. MUÑOZ^{2,3}¹ *Departamento de Física da Faculdade de Ciências e Centro de Física da Matéria Condensada da Universidade de Lisboa, Avenida Professor Gama Pinto, 2, P-1643-003 Lisboa Codex, Portugal*² *Depto. de E. y Física de la Materia, Universidad de Granada, 18071 Granada, Spain*³ *Institute Carlos I for Theoretical and Computational Physics, University of Granada, 18071 Granada, Spain.*

(received ; accepted)

PACS. 05.70.Fh – Phase transitions general studies.

PACS. 68.45.Gd – Depinning.

Abstract. – We study a Langevin equation describing non-equilibrium depinning and wetting transitions. Attention is focused on short-ranged attractive substrate-interface potentials. We confirm the existence of first order depinning transitions, in the temperature-chemical potential diagram, and a tricritical point beyond which the transition becomes a non-equilibrium complete wetting transition. The coexistence of pinned and depinned interfaces occurs over a finite area, in line with other non-equilibrium systems that exhibit first order transitions. In addition, we find two types of phase coexistence, one of which is characterized by spatio-temporal intermittency (STI). A finite size analysis of the depinning time is used to characterize the different coexisting regimes. Finally, a stationary distribution of characteristic triangles or facets was shown to be responsible for the structure of the STI phase.

Consider a bulk phase (α) in contact with a substrate. Wetting occurs when a macroscopic layer of a different, coexisting, bulk phase (β) is adsorbed at the substrate. The wetting transition is characterized by the divergence of the wetting layer thickness, *i.e.* the distance between the substrate and the $\alpha\beta$ interface. Equilibrium wetting is a problem of outmost importance. It has been observed experimentally and thoroughly investigated using (among other techniques) interface displacement models [1]. In these models one considers a function $h(\mathbf{x})$ representing the local departure of the interface from a reference plane ($h = 0$) and constructs an effective interface Hamiltonian, $\mathcal{H}(h)$. Using reasonable approximations one arrives at the standard form [1],

$$\mathcal{H}(h) = \int_0^\infty d\mathbf{x} \left[\frac{1}{2} D (\nabla h)^2 + V(h) \right], \quad (1)$$

where D is the interfacial tension of the $\alpha\beta$ interface (or the interfacial stiffness for anisotropic media) $V(h)$ is the external potential accounting for the net interaction between the substrate

and the $\alpha\beta$ interface and \mathbf{x} is a d -dimensional vector. For large values of h at bulk coexistence, the interface potential of a system with short-range forces vanishes exponentially and one writes [1]

$$V(h) = b(T)e^{-h} + ce^{-2h} \quad (2)$$

where h is measured in units of the bulk correlation length ξ , $b \equiv b(T)$ vanishes linearly with $T - T_W$, where T_W is the (mean-field) wetting transition temperature and $c > 0$. At sufficiently low temperatures, $b < 0$, the potential V binds the $\alpha\beta$ interface, that is, the equilibrium thickness of the wetting layer $\langle h \rangle$ is finite. As the temperature is raised, the potential becomes less attractive and at bulk coexistence it no longer binds the interface; $\langle h \rangle$ diverges. In this regime, a linear term μh , where μ is the chemical potential difference between the α and β phases, may be added to $V(h)$ to study complete wetting [1].

A dynamic generalization of the equilibrium wetting models is given by the following Langevin equation

$$\partial_t h(\mathbf{x}, t) = D\nabla^2 h - \partial V / \partial h + \eta(\mathbf{x}, t), \quad (3)$$

where η is a zero-mean Gaussian white noise. This was introduced by Lipowsky [2], and describes the relaxation of h towards its equilibrium distribution. In this context, μ plays the role of an external force acting on the interface. In the absence of the substrate, $\mu = 0$ guarantees that the mean velocity of the interface is zero regardless of its average position, $\langle h \rangle$, as required by bulk coexistence.

The dynamic model is readily generalized to non-equilibrium interfacial processes, *e.g.*, crystal growth, atomic beam epitaxy, etc., where thermal equilibrium does not apply. An effective non-equilibrium interfacial model consists of a Kardar-Parisi-Zhang (KPZ) equation [3] in the presence of a substrate. Consider the free interface that is solution of the KPZ equation. A depinning transition occurs at a chemical potential, $\mu = \mu_c$, that depends on the strength of the KPZ non-linearity. The non-equilibrium analogous of complete wetting corresponds to a depinning transition, that occurs at $\mu = \mu_c$, in the presence of the substrate.

A discrete model that exhibits this type of transitions was introduced in [4]. Interfacial growth was analyzed for a model with adsorption/desorption rules that violate, in general, detailed balance. It was shown [4] that the corresponding effective interface model is a KPZ equation in the presence of a repulsive external potential. Under equilibrium conditions, the KPZ nonlinearity vanishes [4] and the model reduces to that of equilibrium wetting [2]. The difference between the adsorption and desorption rates plays the role of a driving force (analogous to the chemical potential difference, μ), and controls the mean velocity of the interface. For repulsive substrates, a depinning or complete wetting transition was shown to occur at $\mu = \mu_c$, the value where the mean velocity of the free interface vanishes. Under equilibrium conditions the KPZ non-linearity vanishes and a complete wetting transition occurs at $\mu_c = 0$. An earlier study of non-equilibrium complete wetting was based on the KPZ equation [3] in the presence of a *hard wall* [5]. It was shown [5, 4], that this non-equilibrium transition exhibits scaling properties characterized by the KPZ exponents, in addition to those associated with the pinned phase, that are described by new critical exponents. It was also established that there are two universality classes determined by the sign of the KPZ non-linearity [5, 4].

Subsequently, the effect of short-range attractive substrates was studied for the discrete model [6]. It was found, that for sufficiently attractive substrate potentials, the depinning transition becomes first-order and that, by contrast with equilibrium systems, at a given temperature there is a finite range of chemical potentials for which phase coexistence occurs. These results were confirmed by Giada and Marsili [8] using a KPZ equation in the presence of

an attractive substrate. In contrast with the transitions that occur for repulsive substrates the first-order transition is not driven by the (attractive) substrate. Here we carry out extensive studies of a similar KPZ equation, using mean field techniques and numerical simulations for repulsive and attractive substrate potentials. Some of our results for the first-order transition are similar to those of [8, 9] while others are new, namely the existence of spatio temporal intermittency (STI), facets, and two distinct regimes in the coexistence region. We argue that the continuous transitions that occur for repulsive substrates are non-equilibrium complete wetting; in addition, we discuss the nature of the first order depinning transitions that occur in the presence of attractive substrates.

The model – We consider a KPZ equation with a substrate potential given by $V(h) = -(a+1)h + be^{-h} + ce^{-2h}/2$ with $c > 0$ [8],

$$\partial_t h(\mathbf{x}, t) = D \left[\nabla^2 h - (\nabla h)^2 \right] - \frac{\partial V(h)}{\partial h} + \eta. \quad (4)$$

$a+1$ acts as a chemical potential difference between the two phases and b is the temperature measured with respect to the (mean-field) equilibrium wetting transition temperature. Thus for $b > 0$ this equation describes non-equilibrium complete wetting. For positive values of the KPZ non-linearity, it is easy to show that only second order transitions (in the multiplicative noise, MN, universality class) occur. Performing a Cole-Hopf transformation, $h(\mathbf{x}, t) = -\ln n(\mathbf{x}, t)$, and using Ito calculus the last equation transforms into

$$\partial_t n = D \nabla^2 n - \partial V(n)/\partial n + n\eta, \quad (5)$$

with $V(n) = an^2/2 + bn^3/3 + cn^4/4$, that describes the interfacial problem as a diffusion-like equation with multiplicative noise. In general, any potential of the form $an^2/2 + bn^{p+2}/(p+2) + cn^{2p+2}/(2p+2)$ with $p > 0$ yields an equivalent effective Hamiltonian, since when the last equation is written in terms of h , the parameter p may be set to one through a redefinition of the height variable. The case $p = 2$ (with fixed $b > 0$) has been studied in [9] in the context of stochastic STI. Note that in terms of n the two phases are absorbing (depinned) and active (pinned) respectively, and the critical point signals a transition to an absorbing state [10].

Mean field – In this section we review the mean field analysis of the MN equation. Most of this was presented in [11, 8, 12]; here, we outline the main results. First the MN equation is discretized. In the discretized Laplacian, the sum of the nearest-neighbor field values is replaced by the average value of the field, $\langle n \rangle$, and a closed Fokker-Planck equation is obtained for $P(n, t, \langle n \rangle)$. This equation is solved self-consistently, by equating the average value of n , $F(\langle n \rangle)$, with $\langle n \rangle$. Except for the limiting cases $D = 0$ and $D = \infty$ where analytical solutions exist, [12, 9, 8] the self-consistency equation is solved numerically.

Setting (without loss of generality) $D = 2, c = 1.5$ and $p = 2$, three different regimes were found for $b < 0$ (Fig.1): (i) Depinned phase: one stable solution, $n = 0$ (dash-dotted line); (ii) Coexistence: two stable solutions and one unstable (dashed line); (iii) Pinned phase: one unstable solution, $\langle n \rangle = 0$, and one stable, $\langle n \rangle \neq 0$ (solid line). For positive values of b only regimes (i) and (iii) are found, consistent with the continuous nature of the complete wetting transition. The associated phase diagram is depicted in Fig. 1. The solid line is the continuous phase boundary between depinned and pinned phases. In the region delimited by the dashed lines, both of which correspond to first-order boundaries, the depinned and pinned phases coexist as stationary solutions of the dynamical equation. The three lines meet at the (mean-field) tricritical point $a = 0$ and $b = 0$.

Beyond mean-field theory – We have verified by means of extensive numerical simulations that a phase diagram analogous to that of Fig. 1 survives the effects of fluctuations. The phase boundaries were located by fixing b and tuning a . For large (positive) values of b the

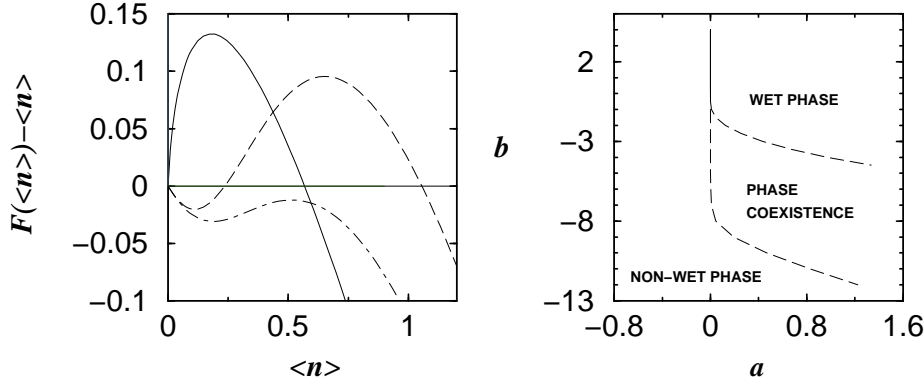


Fig. 1. – Typical solutions of the equation $F(\langle n \rangle) = \langle n \rangle$ for different values of a , and mean-field phase diagram.

transition is found to be continuous. Mean-field results are expected to hold at this transition above the upper critical dimension $d_c = 2$ [5]; in fact, if $b > 0$ and $d > 2$, the term n^{2p+2} is irrelevant in the renormalization group sense, and we are left with the *multiplicative noise* equation studied in [5, 10]. For completeness, we have calculated the order parameter critical exponent, β , in dimensions above and below d_c . In $d = 1$ ($d = 3$) we found $\beta = 1.65 \pm 0.05$ ($\beta = 0.96 \pm 0.05$) in agreement, within error bars, with the prediction for the MN class [5, 12].

Let us now focus on the first order transition. We fixed (without loss of generality) $p = 2$, $b = -4$, $c = 1.5$, $D = 2$. For these values of the parameters a first order transition is expected at the mean field level. In order to establish the phase boundaries, we performed numerical simulations for one-dimensional systems with system sizes up to $L = 2000$, starting the runs with two different types of initial conditions (IC): (1) Pinned interfaces with typical values of h close to the wall, or equivalently $n = 1$, *i.e.*, in the active regime. We refer to this as ‘pinned’ IC. (2) Depinned interfaces with large values of h (small values of n , close to the absorbing state $n = 0$). In general, an interface is considered detached from the substrate when all the values of $h(\mathbf{x})$ are positive ($n(\mathbf{x}) < 1$, $\forall \mathbf{x}$). First, we have verified that the depinned phase is stable for values of a larger than $a \sim 0$. The behavior for pinned IC, however, is much harder to analyze due to finite size effects: for any finite size the only stationary state is the depinned (absorbing) one. Thus, in order to establish the stability of the pinned phase, one has to perform a finite size analysis of the characteristic time needed for a system with pinned IC to depin [6]. We have measured these times in two different ways: (i) the time τ that characterizes the exponential decay of $\langle n(t) \rangle$, averaged over all runs ($\forall a$), after a short transient; and (ii) the time needed for the last site in the interface to detach ($n(\mathbf{x}) < 1$, $\forall \mathbf{x}$). Both lead to the same qualitative results. We observed three regimes:

(1) For $a \lesssim 1.22$ there is an exponential growth of τ as $L \rightarrow \infty$, implying that the pinned state is stable in the thermodynamic limit. As the depinned phase is stable for $a \gtrsim 0$ the system exhibits coexistence of the depinned and pinned phases in the range $0 \lesssim a \lesssim 1.22$ in analogy with other nonequilibrium systems [7]. Note that owing to the huge characteristic times in this regime, obtaining good statistics, even for relatively small systems, is prohibitive. Within error-bars, however, the overall behavior is compatible with an exponential.

(2) In the range $\approx 1.22 \lesssim a \lesssim 1.3$ an approximate power-law dependence is found, at least for the accessible system sizes (see Fig. 2A). The pinned phase is stable as τ tends to infinity, in the infinite size limit. Note also the presence of a step separating two different regimes (see

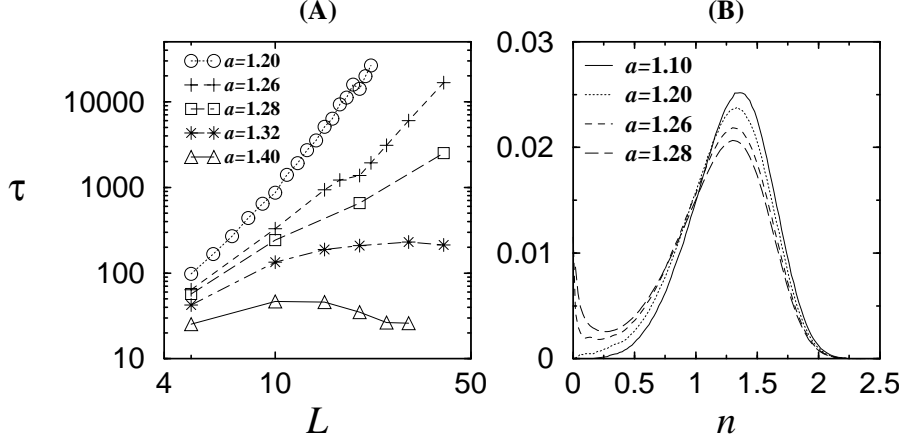


Fig. 2. – Characteristic times for the decay of $\langle n(t) \rangle$ and single site (unnormalized) pdf for different values of a .

curve for $a = 1.26$ in Fig. 2); this step has the same origin as the maximum in the curves of the third regime to be discussed below. Much larger simulations, inaccessible to the available computing power, are required in order to establish whether (i) these power laws describe the true asymptotic behavior, (ii) for very large systems they become exponentials and (iii) the power-law region shrinks to a line. The CPU time required to measure τ accurately, for large L , is huge as the distribution of detaching times is very broad.

(3) For $a \gtrsim 1.3$, τ tends to a constant, *i.e.* in the thermodynamic limit, the system is depinned in a finite time. Note in Fig. 2 the rather unusual dependence on the system size. For instance, for $a = 1.4$ the curve has a maximum around $L = 11$, and then decays monotonically. This means that the interface is more easily detached in a large system than in a smaller one, which is counterintuitive. This can be rationalized by considering on the one hand a depinning ‘zipper’ mechanism: once a site is detached it pulls out its neighbors, and they in turn pull out their neighbors, and so on, until (if the system is small enough) the whole interface is depinned (in a time which grows linearly with L). The existence of this mechanism was verified numerically. On the other hand, the larger the system size L , the larger the probability of a fluctuation that detaches a single site. The competition of these two mechanisms is responsible for the non-monotonic behavior of the characteristic times in the third regime (as well as for the step in the previous regime).

To clarify the nature of the second regime we performed further analysis. Fig. 3A, depicts a typical spatio-temporal snapshot of the field n , for $a = 1.28$. Patterns characteristic of STI [9] are observed in this regime (and only in this regime). The pattern is characterized by the simultaneous presence of pinned and depinned patches, and the distribution of the latter is rather broad. This regime was unnoticed in previous studies of non-equilibrium depinning transitions [11, 8]. STI occurs for a narrow set of parameters only and not generically in the pinned phase, contrary to a previous suggestion [9]. In fact, the different exponential and power-law regimes, in the coexistence region, was unnoticed in that work [9]. Roughly speaking the STI regime, where statistically stationary patches of depinned and pinned regions are seen in generic configurations, coincides with the second or power-law regime reported in this work.

In order to quantify the distinction between the STI and the non-STI (globally) pinned

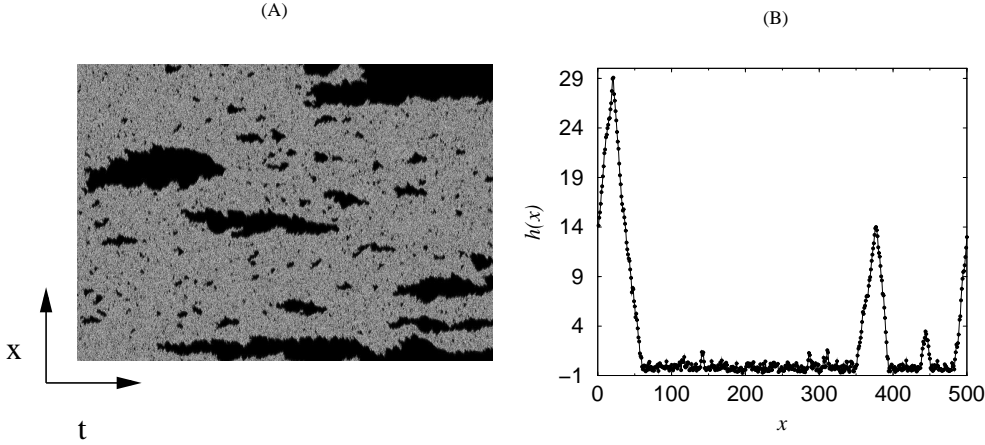


Fig. 3. – A. Snapshot for $a = 1.28$; (dark = depinned, $n < 1$; grey = pinned, $n > 1$). Islands of very different sizes of the minority phase are ubiquitous. The 1000 depicted time slices were taken at intervals of 50 time units. $L = 500$. B. Typical configuration of h corresponding to the time slice 400, marked with a line in the previous snapshot.

phases, we have studied the single site probability distribution function (ss-pdf). The ss-pdf was introduced in [10] as a suitable tool to distinguish between different absorbing states. Instead of averaging $n(t)$ over all runs, as before, we average only over the pinned (surviving) runs starting from pinned IC. This yields non-trivial stationary values of $\langle n \rangle$ in the first two regimes, while in the third the only stationary state is $n = 0$. For small values of a ($a \lesssim 1.22$) the stationary histogram is bell-shaped (see Fig. 2B). For a slightly larger than 1.22 (*e.g.* 1.26 or 1.28) the ss-pdf retains its bell-shape while developing a second peak around $n = 0$. The relative height of the two peaks changes continuously as a increases. At a certain value of a , signaling the first order transition, the peak at zero n increases dramatically and the pinned phase becomes unstable. Physically, a large number of depinned islands is generated that eventually coalesce and depin the interface. Consequently, the STI is restricted to a narrow region below the first order boundary where the two peaks of the stationary ss-pdf co-exist, or in other words, where detached patches are generated but are suppressed in times comparable to the typical coalescence time [6]. A typical configuration of h in the STI regime ($a = 1.28$) is shown in Fig. 3B. Note the presence of triangles analogous to those described in [6]; in fact, the mechanism responsible for these triangular facets, is similar to that described in [6], though here, there is no height-gradient constraint. The (average) slope of each triangle, s , is a constant (modulo fluctuations), and may be determined from the condition $\lambda_R s^2 = a + 1$, where the renormalized value of the non-linear coefficient λ_R is measurable by globally tilting the interface [3, 13]. Similar triangles, have been reported for the Frenkel-Konroutova equation [14] and for the KPZ dynamics with negative non-linearities in the presence of quenched disorder [13].

Summing up, we have studied a general Langevin equation describing non-equilibrium interfacial phenomena, for short-range interactions between the interface and the substrate. We have found, that the non-equilibrium transitions may be continuous or first order. The former are complete wetting transitions driven by the repulsive substrate while the latter correspond to the non-equilibrium growth of an interface driven by the chemical potential difference. In the first-order regime there is coexistence between pinned and depinned interfaces for a finite

range of parameters. Thus, the approach to the critical wetting transition ($a = b = 0$ within mean-field) may be realized along different paths, within the finite coexistence region (delimited by dashed lines in the mean-field diagram of Fig. 1). Moreover, within the coexistence region there are two sub-regimes: one exhibiting STI (characterized by a two-peaked ss-pdf) and one with a more standard pinned phase (with no STI and a bell-shaped ss-pdf). In the former the characteristic times grow with L (roughly) in an algebraic fashion, while in the latter the growth is exponential. Finally, we have reported on the existence of triangular structures or facets in one-dimensional interfaces.

Several important issues remain open and should be addressed before a connection with experiments is made. The key task is that of developing criteria to determine whether the KPZ non-linear term should be included in the effective interface Hamiltonian of a given system. The KPZ nonlinearity describes lateral growth, a mechanism that is unlikely to be relevant for fluid interfaces, but may determine the (anisotropic) growth behavior observed in crystals [15] at least in systems with short-ranged interactions. In addition, it remains to be checked whether the phenomenology described here survives in higher dimensions and/or the presence of long-ranged interactions. Finally, the crossover between non-equilibrium wetting transitions and equilibrium wetting, i.e., the weak coupling limit of the KPZ equation in the presence of a substrate, remains a challenging theoretical problem. By analogy with short-ranged equilibrium wetting, it is expected that the study of non-equilibrium critical wetting will reveal the existence of new universality classes, that may depend on the path within the finite coexistence region.

Acknowledgments – We acknowledge partial support from the European Network contracts ERBFMRXCT980183 and ERBFMRXCT980171, the Spanish DGESIC project PB97-0842 and a running grant of the FCT (Portugal) under their Pluriannual Programme.

REFERENCES

- [1] See, S. DIETRICH, *Phase Transitions and Critical Phenomena*, vol. 12, ed. by C. Domb and J. Lebowitz, Academic Press, 1988. D.E. SULLIVAN AND M.M. TELO DA GAMA, in *Fluid Interfacial Phenomena*, ed. C.A. Croxton. Wiley, New York, 1986 and references therein.
- [2] R. LIPOWSKY, *J. Phys. A*, **18** L585 (1985).
- [3] A. -L. BARABÁSI AND H. E. STANLEY, *Fractal Concepts in Surface Growth*, Cambridge University Press, Cambridge, 1995. T. HALPIN-HEALY AND Y.-C. ZHANG, *Phys. Rep.*, **254** 215 (1995).
- [4] H. HINRICHSSEN, R. LIVI, D. MUKAMEL, AND A. POLITI, *Phys. Rev. Lett.*, **79** 2710 (1997).
- [5] M.A. MUÑOZ AND T. HWA, *Europhys. Lett.*, **41** 147 (1998). G. GRINSTEIN, M.A. MUÑOZ AND Y. TU, *Phys. Rev. Lett.*, **76** 4376 (1996). Y. TU, G. GRINSTEIN AND M.A. MUÑOZ, *Phys. Rev. Lett.*, **78** 274 (1997).
- [6] H. HINRICHSSEN, R. LIVI, D. MUKAMEL AND A. POLITI, *Phys. Rev. E*, **61** R1032 (2000).
- [7] A. L. TOOM, *Multicomponent Random Systems*, ed. by R. L. Dobrushin, in *Advances in Probability*, Vol. 6 (Dekker, New York), 1980. C. H. BENNETT AND G. GRINSTEIN, *Phys. Rev. Lett.*, **55** 657 (1985).
- [8] L. GIADA AND M. MARSILI, *Phys. Rev. E*, **62** 6015 (2000).
- [9] M.G. ZIMMERMANN, R. TORAL, O. PIRO, AND M. SAN MIGUEL, *Phys. Rev. Lett.*, **85** 3612 (2000).
- [10] M. A. MUÑOZ, *Phys. Rev. E*, **57** 1377 (1998).
- [11] R. MÜLLER, K. LIPPERT, A. KÜHNEL, AND U. BEHN, *Phys. Rev. E*, **56** (1997) 2658.
- [12] W. GENOVESE AND M.A. MUÑOZ, *Phys. Rev. E*, **60** 69 (1999).
- [13] H. JEONG, B. KAHNG AND D. KIM, *Phys. Rev. E*, **59** 1570 (1999).
- [14] T. STRUNZ AND F. J. ELMER, *Phys. Rev. E*, **58** 1601 (1998).
- [15] J. VILLAIN, *J. Phys. I*, **19** 1 (1991). A. PIMPINELLI AND J. VILLAIN, *Physics of Crystal Growth*, Cambridge University Press, New York, 1998.